

Computed structures and energetics of ionic neon clusters using DFT correlation corrections

F.A. Gianturco^a and F. Sebastianelli

Department of Chemistry, The University of Rome, Città Universitaria, 00185 Rome, Italy

Received 30 December 1999 and Received in final form 29 February 2000

Abstract. The structural properties of some of the smaller ionic clusters of neon atoms are examined at the post-Hartree-Fock level using a variety of correlation corrections described within a Density Functional treatment. The results of the calculations, and the physical reliability of the method, are discussed in comparison with earlier theoretical results and with the scanty experimental data. The possible presence of a dimeric ion as the core ionic moiety of all the clusters is indicated by the present treatment which also underlines the weaker binding of the outer “shells” of Ne atoms to the central moiety and the rather marked overall charge localization into the central ionic core of the clusters.

PACS. 36.40.-c Atomic and molecular clusters – 71.24.+q Electronic structure of clusters and nanoparticles – 61.46.+w Clusters, nanoparticles, and nanocrystalline materials

1 Introduction

The interaction between neutral rare gas atoms, in their electronic ground state, is in principle of a simple nature since they have closed-shell configurations and are unable to form conventional chemical bonds. Furthermore, the monomeric electronic bound states exhibit spherical symmetry and the neighbouring excited states are usually Rydberg-like in nature. They are therefore fairly different both structurally and energetically. Hence, the configurations of the molecules, clusters, liquids and solids formed by rare gas atoms as building blocks are mainly determined by their atomic “size”, their long-range attractive interactions (the van der Waals (vdW) forces) and the interplay of these two main features [1–3]. The interactions become naturally more complicated when other kinds of “impurity” (atomic or molecular) are added to the rare gas (Rg) clusters although, except for some special cases, such interactions do not significantly alter the electronic structure of the Rg monomers [4,5].

On the other hand, the features of the aggregates of Rg atoms are changed dramatically if one of the outer electrons is removed from any of the closed-shell electronic structures as the result of cluster ionization or excitation. The ensuing Rg atom (or subset of Rg atoms) with an electron deficiency in the outer shell becomes chemically active and is therefore able to form strongly bound molecular-type of structures whose description from a theoretical and computational standpoint often becomes more intricate than that of vdW clusters. We know, in fact, that the processes mentioned above can give rise to a broad variety of final states from a given initial system depending on whether conventional molecular

and cluster ions are directly formed or the neutral aggregate undergoes first excitation into Rydberg-like states or instead electron-transfer complexes are formed by migration from one of the Rg atoms into one of the impurities in the cluster. What the above final channels have in common, however, is the fact that most of their properties are determined to a great degree by the properties of the rare gas ionic cores which are formed as initial states. However, in spite of the extensive studies, both experimental and theoretical, which exist for ionic Rg clusters, there are several aspects of their structural properties (and of their microscopic energetics) which are still not fully clarified. Even for the case of the smaller clusters Rg_n^+ , with $n \leq 20$, the experimental evidence does not allow one to choose without any doubt definitive electronic and geometric structures. Thus, clear-cut answers to questions regarding

- (i) the ionic moiety that is formed after the initial process;
- (ii) the structure of the latter and its ground state, stable geometry;
- (iii) the formation of further Rg shells surrounding the central moiety and their possible structures;
- (iv) the sequential behaviour of stabilization energies as a function of cluster size and the likely appearance of “shell structures” or of “magic” numbers in the series of n values;
- (v) the localized nature of the initial charge (either negative or positive) and the likelihood of it being able to define the presence of a definite ionic moiety that keeps its structure along the cluster growth;

have been considered for several types of Rg_n^+ cases but only answered partially and as yet fairly incompletely [6–8].

^a e-mail: fagiant@caspur.it

In the present study we have therefore decided to examine in some detail, and from theoretical and computational standpoints, the behaviour of the small ionized clusters of neon atoms by searching for their most stable structures, the energetics of the cluster growth after the initial ionization and the most likely ionic core which is able to provide, within the present treatment, the accretion center for the examined structures. Similar studies on Ne_n^+ ionic aggregates have been carried out before [9,10] and they have invariably involved some approximate handling of the interaction forces. It therefore becomes of interest to see how some of the recently developed *ab initio* Density Functional (DFT) approaches could be successfully employed to treat the title systems as supermolecular, all-electron structures and how they compare with the earlier findings.

In the following section we briefly outline our computational method while in Section 3 we present our results and compare them with earlier calculations and with other findings on Ne_n^+ structural properties. Our final conclusions are presented in Section 4.

2 The density functional models

The basic idea underlying the development of the various DFT formulations is the hope of reducing complicated, many-body problems to effective one-body problems. The earlier, most popular approaches have indeed shown that a many-body system can be dealt with statistically as a one-body system by relating the local electron density $\rho(\mathbf{r})$ to the total average potential, $V(\mathbf{r})$, felt by the electron in the many-body situation. Such treatments, in fact, produced two well-known mean-field equations, *i.e.*, the Hartree-Fock-Slater (HFS) equation [11] and the Thomas-Fermi-Dirac (TFD) equation [12]. It stemmed from such formulations that to base those equations on a density theory rather than on a wavefunction theory would avoid the full solution of an eigenvalue problem and aim instead at a global knowledge of the nature of the molecular electronic ground states [13].

In the last 20 years the DFT approach has therefore emerged as a powerful tool for the analysis of a large variety of atomic and molecular systems [14–16], and it is now beginning to appear as an interesting alternative to more extensive (and expensive) treatments based on many-body-perturbation-theory (MBPT) expansions.

In particular, we wish to examine in some detail the reliability and quality of computed, relative stabilization energies of different optimized geometries in ionic clusters of neon when adding correlation energy contributions to the standard static + exchange + distortion interactions given by any self-consistent field (SCF) calculation employed within the average potential approach of the Hartree-Fock (HF) model. We will therefore consider several different forms of correlation contributions which stem from a DFT estimate for such quantities [17].

More recent treatments within the DFT formalism include the exchange approximation suggested by Becke [18], which contains a parametric correction for the asymp-

totic behavior of a localized functional and also includes a gradient-corrected DFT approximation for exchange energies. Such an approach was further modified over the years [19,20] by fine-tuning the parametric choices in the exchange term and by including dynamical correlation effects using the local spin density approximation (LSDA).

The additional correlation energy correction is an important effect that brings energy calculations beyond the HF approach and has been discussed many times within the DFT approach, especially within the context of local density approximations (LDA) [21]. In particular, we have found [22] that, even when dealing with the more complicated problem of dynamical correlation effects in electron scattering processes, an effective description of correlation forces comes from a DFT parameterization of them that includes gradient corrections and was proposed by Lee, Yang, and Parr [23] by optimizing the parameters to the exact value of the correlation energy in the He atom. We will call it here the E_c^{LYP} correlation correction. The actual analytic expression for it was also given already many times [23,24] in the literature and will not be repeated here.

A slightly simpler form of DFT functional in local form to treat correlation energy corrections was introduced a while ago by Perdew and Zunger [25] who essentially employed a modified version of the free-electron-gas (FEG) treatment of Kohn and Sham [14]. When tested for electron scattering processes [22], it essentially agreed with the results that used the original FEG modeling of correlation forces. We will call it the E_c^{PL} contribution. A further gradient correction to this correlation energy will be called E_c^{P86} [26] and will be employed in the present study.

Another, earlier formulation of correlation energy correction was put forward a while ago by Vosko *et al.* [27] by using Padé approximation techniques to accurately interpolate Monte Carlo results for the densities of atoms, molecules, and metals [28]. They found that the ensuing numerical formulae produce a correlation energy, E_c^{VWN} , which has an estimated maximum error of $\sim 10^{-3}$ Rydbergs [27]. It will also be tested and discussed below. In conclusion, the present work will be considering four different forms of correlation energy corrections which have been recently discussed in the literature and some of which have also been tested by us in earlier scattering calculations: the E_c^{LYP} form [23], the E_c^{P86} form [26], the E_c^{VWN5} form [27] and the further correlation energy labelled E_c^{PW91} , discussed in the literature in reference [29] as a modification to E_c^{PL} [25].

It is important to note now that the above functional forms will be used by us in the formulations implemented within the GAUSSIAN 94 package of codes [30]. This means, therefore, that the post-Hartree-Fock correlation corrections will be handled slightly differently from their specific expressions quoted in the original literature outlined before. It is worth mentioning, in fact, that the above LYP prescription contains now a further “tuning” of the types of correlation formulae which it can use by selecting an admixture of gradient-corrected and local correlation

expressions. Furthermore, the corresponding E_c^{PW91} implemented in reference [30] uses the correlation correction discussed before and labelled E_c^{PL} and adds to it a further correlation correction introduced by Perdew in 1992 [29]. It is also interesting to note that we have used similar forms for the DFT correlation energy corrections to HF results to treat the anisotropic, short-range neutral interaction of He atoms with molecular system [31] and found that such effects were well described by the formulation of the E_c^{LYP} discussed before.

As mentioned in the introduction, the calculations were initially carried out by using the well-known “clamped nuclei” approximation for the nuclear dynamics which is the basis for the Born-Oppenheimer (BO) decoupling approach. The actual basis set chosen was the one corresponding to an extended expansion with polarization functions which is usually labelled by the acronym 6-311+G* in the current literature [30].

Furthermore, in order to afford a realistic treatment of the more weakly bound, outer partners of the cluster we have examined some of the structures (see below) by using a simple harmonic approximation for the “breathing” mode in each aggregate in order to estimate the lowest bound vibrational states and therefore the corresponding Zero Point Energy (ZPE) corrections. In spite of the physical simplicity of such a treatment, we shall show below that this correction is already giving us some idea about the effect of nuclear delocalization on protonated clusters, an aspect which we have recently analysed using *ab initio* Molecular Dynamics (CPMD) for both helium and argon [32]. One should keep in mind, however, that the marked quantum nature of the weak bonding forces existing in such systems, and therefore the delocalized positioning of each Ne atom bound to the ionic moiety, makes the use of the above harmonic approximation only of qualitative help in understanding ZPE effects in these systems.

3 Present computational results

In the Rg_n^+ ($n \leq 20$) clusters, the charge is generally supposed to be localized at an ionic core containing a few Rg atoms. This ionic core is in turn surrounded by neutral or almost neutral further Rg atoms which are attracted by polarization forces and, to a lesser degree, by dispersion forces to the charged moiety provided by that core. The main problem which has been intensively discussed in many experimental and theoretical studies [32–35] is the size and structures of such ionic cores. The simplest model of one atomic ionic core is, generally speaking, somewhat unrealistic since the Rg^+ ions are chemically active and are well able to form stable diatomic molecules Rg_2^+ or small Rg_n^+ units where charge is shared by all the component atoms. Although in the gas phase the Rg_n^+ clusters with $n > 2$ are often more stable than the $\text{Rg}_2^+ \dots \text{Rg}_{n-2}$ clusters, their relative stability inside a larger cluster is not at all obvious as the energy provided by the polarization and dispersion forces between the ionic cores and the neutral atoms (and between the neutral atoms themselves) is of the same order as the cluster dissociation energies. Furthermore, the delocalization of the charge on more atoms

decreases the system energy but decreases also the stabilizing effects from the attractive polarization forces, a fact which therefore imposes spatial limits on the charge spread, as we shall see below.

To begin with a general assessment of the quality of our post-Hartree-Fock treatment of correlation correction, we show in Table 1a, lower panel, the computed total energies of the ground electronic states of the neutral Ne atom and of its lowest ionic configuration, Ne^+ . We also show there the values of the computed dipole polarizabilities. As one can see, all the computed values are smaller than the experiment, suggesting a weaker polarization interaction of the neutral added atoms to the ionic core. On the other hand, as we further discuss below, the size of the clusters which we are considering here allow us not to employ the asymptotic interaction as the sole binding force to that core. It is also interesting to note that the DFT calculations for the neon atom polarizability which use the Half + Half model [30,31] yield a larger value of $1.513a_0^3$, in better accord with experiments. The four different calculations refer, as mentioned before, to the E_c^{LYP} correction [23], to the E_c^{P86} correction [26], the correlation correction of E_c^{PW91} [29] and the E_c^{VWN5} correction [27]. The correlation correction which produces the largest change from the pure HF results is the E_c^{VWN5} , with the E_c^{P86} also giving a very marked energy lowering. As a comparison, the total energy was computed for the Ne atom using a fully correlated, Coupled cluster (CCSD) approach [36] and the calculations were carried out with different basis set sizes (see Tab. 1b). One sees there that the CCSD energy values are higher than those given by the DFT treatments. Correspondingly, the total energy of the ground state of the Ne^+ ion obtained with the same CCSD method yields a value again higher than that from the DFT calculations. It therefore follows that the total energies of the dimeric ion, shown in the upper part of the same Table 1, although optimized in terms of internuclear distances and including also the ZPE corrections (values which were, on the average, around 41 meV ($\sim 330 \text{ cm}^{-1}$)) yields a dissociation energy ΔE that is smaller than that given by the CCSD results of Table 1b. It is worth mentioning however, that the corresponding ZPE value is fairly close to the one computed using multireference configuration interaction calculations: $\sim 350 \text{ cm}^{-1}$ [37], while an earlier computation [38] yielded 253 cm^{-1} .

The experimental dissociation energies for the Ne_2^+ vary from 1.1 eV to 1.35 eV [39,40]. The computed ΔE value of reference [37] was 1.35 eV, while the present values, listed in the last column on the upper panel of Table 1a and in Table 1b, are rather disappointingly small. The most recent calculations [10] which employed the Molpro suite of codes [41], found a value of 1.41 eV. The equilibrium geometry found in reference [37] was 1.73 Å, while the more recent calculations [10] indicated it to be about 1.70 Å. The present results are therefore in good accord with such findings as they range in Table 1a from 1.68 to 1.70 Å. Also our computed dissociation energy values in the lower part of Table 1b are in good accord with the earlier findings.

Ne_2^+	r	E	ZPE	$E(incl.ZPE)$	$\Delta E(eV)$
$E_x^{HF} + E_c^{LYP}$	1.687	-257.062666	0.00151	-257.061155	0.418 0.377
$E_x^{HF} + E_c^{P86}$	1.680	-257.067244	0.00153	-257.065716	0.364 0.323
$E_x^{HF} + E_c^{PW91}$	1.684	-257.054091	0.00151	-257.052583	0.294 0.253
$E_x^{HF} + E_c^{VWN5}$	1.702	-257.759988	0.00145	-257.758537	0.218 0.178

	E (Ne atom)	E (Ne ion)	$\alpha_0(a.u.)^*$
$E_x^{HF} + E_c^{LYP}$	-128.910163	-128.137123	0.900
$E_x^{HF} + E_c^{P86}$	-128.915852	-128.138000	0.873
$E_x^{HF} + E_c^{PW91}$	-128.908751	-128.134531	0.870
$E_x^{HF} + E_c^{VWN5}$	-129.273148	-128.478844	0.872

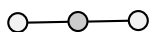
*experimental Ne polarizability = 2.67 a.u.

(a)

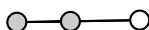
	Ne_2^+	$Ne Atom$	Ne^+	$\Delta E(eV)$
$E_x^{HF} + E_c^{LYP}$ $AUG - cc - pVTZ$	-257.082920 $R_e = 1.655$	-128.916928	-128.146959	0.518
$E_x^{HF} + E_c^{LYP}$ $AUG - cc - pV5Z$	-257.111480 $R_e = 1.654$	-128.930383	-128.161661	0.529
$E_x^{HF} + E_c^{LYP}$ $cc - pV6Z$	-257.112023 $R_e = 1.654$	-128.930668	-128.161950	0.528
$E_x^{HF} + E_c^{P86}$ $AUG - cc - pVTZ$	-257.088570 $R_e = 1.644$	-128.922611	-128.148834	0.466
$Half\&Half$ $cc - pVQZ$	-256.061421 $R_e = 1.7336$	-128.382176	-127.614142	1.771
$Half\&Half$ $AUG - cc - pVQZ$	-256.062234 $R_e = 1.7349$	-128.382939	-127.614326	1.768
$Half\&Half$ $cc - pV5Z$	-256.068645 $R_e = 1.7341$	-128.386031	-127.617655	1.768
$CCSD$ $cc - pVTZ$	-256.861271 $R_e = 1.723$	-128.798209	-128.017214	1.248
$CCSD(T)$ $cc - pVTZ$	-256.871159 $R_e = 1.725$	-128.802454	-128.019720	1.333
$MP4$ $cc - pVTZ$	-256.872164 $R_e = 1.726$	-128.803166	-128.019371	1.350
$MP4$ $AUG - cc - pVTZ$	-256.888894 $R_e = 1.718$	-128.813790	-128.023629	1.401
$MP4$ $cc - pVQZ$	-256.950134 $R_e = 1.713$	-128.844670	-128.054210	1.395
$MP4$ $cc - pV5Z$	-	-128.859476	-128.066442	-
$MP4$ $cc - pV6Z$	-	-128.864411	-128.070340	-
$BP86(BSSE\ corrected)$ $AUG - cc - pVTZ$	-257.088570 $R_e = 1.644$	-128.922885	-128.149226	0.448
$BLYP(BSSE\ corrected)$ $AUG - cc - pVTZ$	-257.082920 $R_e = 1.655$	-128.917133	-128.147264	0.504
$BLYP(BSSE\ corrected)$ $AUG - cc - pV5Z$	-257.111480 $R_e = 1.654$	-128.930393	-128.161669	0.528

(b)

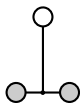
Table 1. (a) Computed total energies (in units of Hartree), relative distances (in Å) and dissociation energies (in units of eV) for the Ne_2^+ dimer (top panel) and for the component atoms (lower panel). The acronyms for the correlation energy corrections are given in the main text. (b) Atomic and diatomic computed total energies using DFT, CCSD and MP4 computational methods and also including BSSE corrections. All calculation acronyms as defined in reference [30].



$Ne_3^+(D_{\infty h})$	$r = r'$	E	ZPE	$E(incl.ZPE)$	$\Delta E(eV)$	$charge$
$E_x^{HF} + E_c^{LYP}$	1.907	-385.976408	0.00117	-385.975237	0.0974 0.107	0.112 0.776 0.112
* $E_x^{HF} + E_c^{P86}$	1.904	-385.984770	-	-	0.0455 -	0.110 0.780 0.110
$E_x^{HF} + E_c^{PW91}$	1.932	-385.964334	0.00105	-385.963286	0.0406 0.0531	0.100 0.800 0.100
$E_x^{HF} + E_c^{VWN5}$	1.986	-387.035225	0.00099	-387.034238	0.0568 0.0695	0.084 0.832 0.084



$Ne_3^+(C_{\infty v})$	r	r'	d'	E	ZPE	$E(incl.ZPE)$	$\Delta E(eV)$	$charge$
$E_x^{HF} + E_c^{LYP}$	1.906	1.908	2.861	-385.976408	0.00117	-385.975237	0.0974 0.107	0.112 0.777 0.111
$E_x^{HF} + E_c^{P86}$	1.710	2.200	3.055	-385.984903	0.00130	-385.983604	0.0492 0.0554	0.034 0.646 0.320
$E_x^{HF} + E_c^{PW91}$	1.748	2.188	3.062	-385.964321	0.00096	-385.963360	0.0402 0.0551	0.038 0.713 0.249
$E_x^{HF} + E_c^{VWN5}$	1.985	1.987	2.979	-387.035225	0.00099	-387.034238	0.0568 0.0695	0.085 0.831 0.084



$Ne_3^+(C_{2v})$	r	d	E	ZPE	$E(incl.ZPE)$	$\Delta E(eV)$	$charge$
$E_x^{HF} + E_c^{LYP}$	1.687	2.394	-385.975460	0.00193	-385.973528	0.0716 0.0601	0.007 0.496 0.496
$E_x^{HF} + E_c^{P86}$	1.679	2.490	-385.984413	0.00186	-385.982553	0.0358 0.0268	0.006 0.497 0.497
$E_x^{HF} + E_c^{PW91}$	1.683	2.580	-385.964014	0.00171	-385.962306	0.0319 0.0264	0.004 0.498 0.498
$E_x^{HF} + E_c^{VWN5}$	1.702	2.705	-387.034238	0.00164	-387.032596	0.0300 0.0248	0.004 0.498 0.498

*= saddle point

Table 2. Same computed quantities (and acronyms) as in Table 1 but for three different configurations of Ne_3^+ . The distance r corresponds to that between atoms in the ionic dimer. The distance d is the one from a Ne partner located in the bisecting plane and the midpoint of the ionic dimer axis. The distance d' is that of a Ne atom along the dimer axis and is taken also to the midpoint of that axis.

We have tried to refine the DFT results by using increasingly larger basis set expansions, by replacing the post-HF treatment with a full DFT approach that includes exchange also (the Half + Half DFT model [30,31]) and we also included the Basis Set Superposition Error (BSSE) corrections to the evaluation of the total energy of the dimer. The results of all our calculations are listed in Table 1b and confirm that the use of DFT methods to yield fixed-nuclei dissociation energies, ΔE , tends to underestimate them when carried out at the post HF level, while is overestimating ΔE when also the exchange contributions are given within the DFT modelling.

The corresponding calculations which we have carried out for the Ne_3^+ system are summarized in Table 2, where the results for three different optimized structures are reported, together with the relative charges which we found to be localized on the atomic components within each calculations.

What we show in the table are the different total energies, the final geometries and the relative ZPE values for the three most stable configurations usually considered with the Rg_3^+ structures, *i.e.* the linear symmetric structure (LS, upper panel), the linear asymmetric structure (LA, middle panel) and the T-shaped triatomic structure

(T, lower panel). For all of them we show post-Hartree-Fock calculations using different correlation models as discussed in the previous section. It is interesting to note at this point that previous studies on the structures and relative stabilities of Rg_3^+ moieties [42–45] and in particular on the Ne_3^+ trimeric unit [37] have discussed at length the relative likelihood of either the LS or LA structures being the most stable configurations. Most of the experimental evidence, however, comes from the study of the near-ultraviolet (UV) bands and of their energy and intensity changes as the cluster size increases [46] where the knowledge of temperature and state population data is very indirect. This means that the ionic moiety can undergo instantaneous deformation due to zero point motion and to possible thermal population of the “other” mode (either symmetric or asymmetric) which is closer in energy. It therefore follows that the existence of a linear symmetric configuration as a possible structure of Ne_3^+ is not necessarily excluded by the experimental evidence, thus making the supporting information from theoretical and computational studies of particular relevance.

In general, we also know that the relative stability of the diatomic and/or triatomic ionic moiety is determined by the dissociation energy of the break-up channel $\text{Rg}_3^+ \rightarrow \text{Rg}_2^+ + \text{Rg}$, which is usually relatively small, *i.e.* around or less than 0.3 eV [47]. In the case of Ne_3^+ , an earlier *ab initio* study that employed Multireference configuration interaction calculations found the dissociation energy into the above channel to be of 0.05, 0.1 and 0.1 eV for the three different equilibrium structures of LS, LA and T, respectively [37]. The suggested experimental value is about 0.1 eV [47]. Earlier theoretical studies employing the diatomics-in-molecule (DIM) method [9] found the trimer ion to have the LA configuration at its equilibrium geometry, and a dissociation energies of about 0.08 eV. The first known calculation [48] on Ne_3^+ reported a linear symmetric structure and a dissociation energy in good agreement with experiments at both the DIM and the *ab initio* levels. Even more recent *ab initio* and DIM calculations [49] of the Ne_3^+ potential obtained the linear symmetric structure, along with a dissociation energy in good accord with experiments. The latest DIM calculations [10] employed a basin-hopping technique [50] to locate the lowest energy minima of Ne_n^+ ($2 \leq n \leq 25$) and confirmed for Ne_3^+ the LS structure with a dissociation energy of 0.107 eV.

The calculations listed in Table 2 suggest the following results:

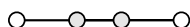
- (i) within the use of the correlation correction previously defined as E_c^{PW91} the LS structure is found to be the most stable, with the LA structure very close in energy. When the ZPE correction is included, however, the LA structure is found in turn to be slightly more stable. In other words, both configurations can exist once the quantum nature of the nuclear bound state is accounted for by going beyond the standard fixed-nuclei (FN) picture;
- (ii) the LS structure yields distances among atoms which are between 1.91 and 1.99 Å (upper panel of Tab. 2),

- while the DIM calculations [10] indicated it to be around 1.85 Å. The earlier *ab initio* results [37] suggested a value of 1.83 Å. The present dissociation energy is of the order of 0.1 eV, in good accord with earlier calculations and with experimental suggestions;
- (iii) the LS indicates, in agreement with the DIM results [10] that very little charge migrates from the wing atoms into the central Ne partner, which shows a positive charge of about +0.8. With the same token, the LA structure indicates (middle panel in Fig. 2) that the Ne_2^+ structure is nearly maintained, with only a 0.03–0.04 positive charge on the third, more distant Ne atom, in keeping with the findings of references [10,37].

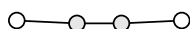
The above considerations appear to suggest that the use of DFT methods for the evaluation of total electronic energies of these cluster ions at the post-Hartree-Fock level is capable of producing reliable data in fair agreement with the earlier calculations. The present results also suggest that the LS trimer structure is very close to the LA configuration and that nuclear vibrational temperatures are an essential piece of information for deciding the physical meaning of selecting one specific, fixed-nuclei configuration as the “most” stable bound shape for the ionic trimer.

In general terms, to account for the structures of Rg_n^+ clusters, where both ionic and neutral species are present due to the fairly strong localization of the positive charge, it is important to be able to include the effects of polarization and of mutually interacting induced dipoles. In the case of Ne its dipole polarizability is relatively small (about $2.56a_0^3$ [51]) and therefore the first-order induction effects are presumably sufficient to describe the surfaces at large relative distances. Our recent calculations on the full potential energy surface using both DFT and more conventional CI methods [52] suggest, in fact, that the first order term becomes dominant beyond about 9–10 Å from the charge location. Therefore, to employ the supermolecular picture within the variational calculation of its post-HF total electronic energy one should correctly include the above effects within the intermediate range of distances which are relevant for the smaller clusters of the present study. We know, in fact, that pure dispersion interaction is not well represented within DFT models which would therefore not be able to describe the far outer Ne shells held together by dispersion forces only.

The examined structures of Ne_4^+ are reported in Tables 3a and 3b, where four of the lowest energy configurations are presented. In all the above structures, as expected, the effect from ZPE correction is more marked than in the case of the trimer. In all the calculations the presence of a “central” ionic moiety which bears more than 90% of the positive charge is clear (see last columns of all panels) and confirms the finding from the latest DIM calculations [10]. Furthermore, the present, global calculations indicate that the most stable structure is not the linear, symmetric tetramer but rather the $\text{C}_{2v}-^2\text{B}_1$ configuration (or the similar C_s configuration for the PW91 correlation correction, see Tab. 3b) with the additional



$Ne_4^+(D_{\infty h})$	r	d'	E	ZPE	$E(incl.ZPE)$	$\Delta E(eV)$	$charge$
$E_x^{HF} + E_c^{LYP}$	1.689	3.141	-514.888446	0.00231	-514.886136	0.0510 0.0200	0.0253 0.0253 0.4747 0.4747
$E_x^{HF} + E_c^{P86}$	1.680	3.202	-514.901925	0.00214	-514.899787	0.0318 0.00901	0.0211 0.0211 0.4789 0.4789
$E_x^{HF} + E_c^{PW91}$	1.683	3.318	-514.874057	0.00203	-514.872023	0.0264 -0.00239	0.0164 0.0164 0.4836 0.4836
$*E_x^{HF} + E_c^{VWN5}$	1.700	3.432	-516.308468	-	-	0.00258 -	0.0130 0.0130 0.4870 0.4870



$Ne_4^+(C_{2v}^{-2}B_2)$	r	d'	θ	E	ZPE	$E(incl.ZPE)$	$\Delta E(eV)$	$charge$
$E_x^{HF} + E_c^{LYP}$	1.689	3.142	177.8	-514.888428	0.00219	-514.886239	0.0505 0.0228	0.0252 0.0252 0.4748 0.4748
$E_x^{HF} + E_c^{P86}$	1.680	3.202	177.8	-514.901921	0.00208	-514.899837	0.0317 0.0104	0.0210 0.0210 0.4790 0.4790
$E_x^{HF} + E_c^{PW91}$	1.683	3.318	177.6	-514.874054	0.00199	-514.872061	0.0264 -0.00136	0.0163 0.0163 0.4837 0.4837
$*E_x^{HF} + E_c^{VWN5}$	1.700	3.433	177.0	-516.308457	-	-	0.00229 -	0.0129 0.0129 0.4871 0.4871

*=saddle point

(a)



$Ne_4^+(C_{2v}^{-2}B_1)$	r	R	d	E	ZPE	$E(incl.ZPE)$	$\Delta E(eV)$	$charge$
$E_x^{HF} + E_c^{LYP}$	1.685	2.638	2.408	-514.888970	0.00248	-514.886495	0.0653 0.0298	0.0069 0.0069 0.4931 0.4931
$E_x^{HF} + E_c^{P86}$	1.678	2.940	2.473	-514.901872	0.00231	-514.899564	0.0304 0.00294	0.0054 0.0054 0.4956 0.4956
$E_x^{HF} + E_c^{VWN5}$	1.700	3.222	2.689	-516.308672	0.00190	-516.306773	0.00814 -0.0167	0.0036 0.0036 0.4964 0.4964
$Ne_4^+(C_s)$	r	R	$d_1 - d_2$	E	ZPE	$E(incl.ZPE)$	$\Delta E(eV)$	$charge$
$E_x^{HF} + E_c^{LYP}$	1.685	2.647	2.402 2.405	-514.888968	0.002486	-514.886482	0.0652 0.0294	0.0070 0.0069 0.4931 0.4931
$E_x^{HF} + E_c^{P86}$	1.678	2.942	2.473 2.473	-514.901846	0.002288	-514.899558	0.0297 0.00278	0.0054 0.0054 0.4946 0.4946
$E_x^{HF} + E_c^{PW91}$	1.681	3.264	2.559 2.574	-514.874178	0.00213	-514.872048	0.0297 -0.00171	0.0043 0.0042 0.4957 0.4957
$E_x^{HF} + E_c^{VWN5}$	1.700	3.244	2.684 2.685	-516.308673	0.001904	-516.306768	0.00816 -0.0168	0.0036 0.0036 0.4964 0.4964

(b)

Table 3. Same computed quantities, and atomic positive charges, as those discussed in Table 2 but for four different configurations for Ne_4^+ . The angle shown in the second panel of (a) gives the distortion from the linear configuration. The additional distances R in (b) represent the relative distances between neon atoms in the bisecting plane.

neon atoms placed on a plane perpendicular to the ionic, dimeric moiety. The latter structure, in fact, gives stabilization energies for the additional atom,

$$\Delta E_e = \Delta E_n - \Delta E_{n-1} \quad (1)$$

$$\Delta E_0 = \Delta E_n^{\text{ZPE}} - \Delta E_{n-1}^{\text{ZPE}} \quad (2)$$

where the ΔE_e corresponds to the total energy difference while ΔE_0 includes also the ZPE corrections, which are the largest for the structures shown *i.e.* 0.06 eV and 0.03 eV, respectively. Both these quantities are given jointly in the columns next to the charge values. These results are in good accord with the values suggested by references [10, 47] where, however, the linear structure was found to be the most stable. The two structures next in energy, *i.e.* the $D_{\infty h}$ and the $(C_{2v}-^2B_2)$ configurations, are both very close in energy with each other and are less stable than the $(C_{2v}-^2B_1)$ or C_s lowest structure by less than 15 meV. We think that the strong localization of the positive charge on the central ionic moiety makes the residual interactions between the nearly neutral first-shell Ne atoms a very important factor. As a consequence of it, the location of the additional neon partners at distances between each other which optimizes the neutral-neutral attractive interaction could be the balancing factor in the search for the minimum energy structures within an FN picture.

A similar behaviour could be gathered from the present results for Ne_5^+ listed in the various panels of Table 4. We show there the comparison between the structural properties of two different C_s geometries with three Ne atoms on the symmetry plane that bisects the ionic dimer. One can make the following comments about the above results:

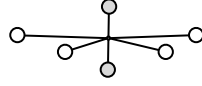
- (i) all calculations, *i.e.* those using two different models for the DFT correlation corrections, indicate the clear presence of an Ne_2^+ moiety with its internuclear distance close to our earlier calculations of Table 1 and for three other neon atoms located at much larger distances from that moiety;
- (ii) the charge remains strongly localized on the dimeric moiety which carries more than 90% of the positive charge, as also indicated by other calculations [9, 10, 47];
- (iii) the ZPE contributions continue to increase, as one should expect, when increasing the size and complexity of the clusters;
- (iv) the most stable structure from the present calculations turns out to be the C_s in the middle panel of Table 4. It indicates that the additional Ne atom locates itself in the same plane perpendicular to the Ne_2^+ moiety where the other two neon partners formed the first shell around the ionic core. However, the fifth additional atoms in that plane, and the C_s configuration, favour distances between nearly neutral Ne atoms which are not far from the equilibrium distance in the Ne_2 interaction (about $5.9a_0$ [53]);
- (v) the one-atom evaporation energy, ΔE_e , given by the use of E_c^{P86} correlation, 0.04 eV, coincides with the latest calculated value [10] using the DIM approach,

while the E_c^{LYP} overestimates correlation effects by giving a ΔE_e value of 0.09 eV. The latter calculations also suggest a similar C_s structure for the ionic pentamer, as was the case from the earlier DIM results [9].

When further increasing the size of the clusters, it becomes of interest to analyse possible competing pathways of accretion around the central ionic moiety, as we have discussed earlier on for the case of protonated Rg clusters [32, 54]. In particular, it is interesting here to see whether the next addition of neon atoms will keep populating the plane bisecting the ionic moiety or will be added to the more external shell along the axis of that moiety. In Tables 5a and 5b we show examples of such comparison for the case of the Ne_6^+ cluster: the former table shows two panels where the calculations of the C_s and C_{2v} symmetries are reported, indicating that to place the four Ne atoms in the plane at similar relative distances from each other and from the axis creates the most stable (C_s) structure for this cluster, in analogy with what we had seen to happen in the Ne_5^+ structure. All the nearly neutral neon atoms in the bisecting plane (see charges in the last columns of tables) have average distances from each other which are close to the minimum of the neutral dimer interaction ($\sim 3 \text{ \AA}$) and they locate themselves from the dimeric moiety at distances that are larger than that of the core: between 2.4 and 2.5 \AA , depending on the chosen correlation model. The chosen model also affects the single-atom evaporation energy, ΔE_e , since its value varies here between 0.046 eV and 0.09 eV, *i.e.* similar to the value found for the Ne_5^+ cluster.

Tables 6 and 7 report the extension of the present calculations to the structures of Ne_7^+ , Ne_8^+ and Ne_9^+ clusters, to further analyse the competitive shell-filling effect mentioned before. In the case of the 7-atom clusters one sees again that filling atoms into the bisecting plane produces the more stable structure in comparison with adding atoms along the ionic axis. Furthermore, one sees that the perfect pentagonal structure of the nearly neutral atoms in the belt of the moiety axis gets slightly distorted into the C_s configuration, thereby producing a slightly more stable structure. The alternative C_s structure with Ne_4^+ containing three further neon atoms in the bisecting plane is, however, slightly less stable than the former by about 3.7 meV and the difference remains the same even when ZPE corrections are considered. Thus, it appears that the present DFT treatment of correlation effects produces the Ne_2^+ core as the more likely moiety for the small ionic clusters.

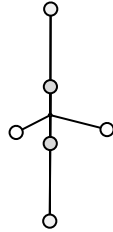
In the case of protonated He clusters, we had found [32, 54] that the ionic moiety was made up of a linear $(He_2H)^+$ molecule with the proton in the middle. The growing process of those clusters also turned out to locate additional He atoms into a bisecting plane up to $n = 5$, while from $n \geq 6$ it was found that the two apex positions of the ionic axis were preferentially occupied. In the present instance something very similar is seen to happen: the results of Table 7 show, in fact, that the most stable structures for Ne_8^+ and Ne_9^+ are of C_s symmetry



$Ne_6^+(C_s)$	r	$R_1 - R_3$	$\frac{d_1 - d_4}{\bar{d}}$	E	ZPE	$E(incl.ZPE)$	$\Delta E(eV)$	$charge$
$E_x^{HF} + E_c^{LYP}$	1.684	2.637 2.654 2.666	2.409 2.404 2.404 2.401 $\bar{d} = 2.404$	-772.716017	0.00365	-772.712365	0.0923 0.0764	0.0071 0.0081 0.0080 0.0072 0.4848 0.4848
$E_x^{HF} + E_c^{P86}$	1.675	2.968 3.374 2.968	2.466 2.453 $\bar{d} = 2.459$	-772.736823	0.00331	-772.733509	0.0463 0.0268	0.0063 0.0058 0.0058 0.0063 0.4879 0.4879

$Ne_6^+(C_1)$	r	$R_1 - R_3$	$\frac{d_1 - d_4}{\bar{d}}$	E	ZPE	$E(incl.ZPE)$	$\Delta E(eV)$	$charge$
$E_x^{HF} + E_c^{LYP}$	1.683	2.627 2.627 2.604	2.426 2.408 2.408 2.426 $\bar{d} = 2.417$	-772.716010	0.00364	-772.712368	0.0921 0.0765	0.0072 0.0083 0.0083 0.0072 0.4845 0.4845
$E_x^{HF} + E_c^{P86}$	1.675	3.318 2.937 2.945	2.455 2.472 2.461 2.457 $\bar{d} = 2.461$	-772.736810	0.00325	-772.733559	0.0460 0.0282	0.0054 0.0061 0.0060 0.0060 0.4882 0.4882

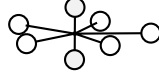
(a)



$Ne_6^+(C_s)$	r	R	$\frac{d_1 - d_2}{d'}$	E	ZPE	$E(incl.ZPE)$	$\Delta E(eV)$	$charge$
$E_x^{HF} + E_c^{LYP}$	1.687	2.650	2.403 2.402 $d' = 3.142$	-772.714818	0.00328	-772.711537	0.0597 0.0539	0.0070 0.0070 0.4678 0.4678 0.0252 0.0252
$E_x^{HF} + E_c^{P86}$	1.678	2.869	2.459 2.468 $d' = 3.205$	-772.736623	0.00293	-772.733693	0.0409 0.0318	0.0055 0.0055 0.4737 0.4737 0.0208 0.0208
$Ne_6^+(C_1)$	r	R	$\frac{d_1 - d_2}{d'_1 - d'_2}$	E	ZPE	$E(incl.ZPE)$	$\Delta E(eV)$	$charge$
$E_x^{HF} + E_c^{P86}$	1.678	2.938	2.469 2.469 3.204 3.205	-772.736594	0.00289	-772.733699	0.0401 0.0320	0.0053 0.0053 0.4732 0.4743 0.0209 0.0208

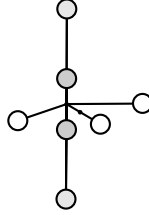
(b)

Table 5. Same computed quantities as in the previous tables but for the different configurations examined for Ne_6^+ . (a) shows the example with four neon partners in the bisecting plane while (b) shows the case with two neon atoms displaced onto the dimeric axis perpendicular to that plane.

Table 6. Same as in Table 5 but for two different configurations for Ne_7^+ ion. See text for the meaning of symbols.

$\text{Ne}_7^+ (D_{5h})$	r	R	d	E	ZPE	$E(\text{incl.}ZPE)$	$\Delta E(\text{eV})$	$charge$
$E_x^{HF} + E_c^{P86}$	1.675	2.896	2.464	-901.654325	0.00350	-901.650820	0.0449	0.0060
							0.0345	0.0061
								0.0061
								0.0061
								0.4848
								0.4848

$\text{Ne}_7^+ (C_s)$	r	$R_1 - R_5$	$\frac{d_1 - d_5}{\langle d \rangle}$	E	ZPE	$E(\text{incl.}ZPE)$	$\Delta E(\text{eV})$	$charge$
$E_x^{HF} + E_c^{LYP}$	1.683	2.669	2.409	-901.629687	0.00419	-901.625493	0.0954	0.0080
		3.459	2.395					0.0076
		2.670	2.395					0.0076
		2.636	2.409					0.0080
		2.636	2.414					0.0073
			$\bar{d} = 2.404$					0.4808
$E_x^{HF} + E_c^{P86}$	1.674	2.934	2.466	-901.654335	0.00358	-901.650750	0.0452	0.0060
		2.931	2.468					0.0060
		2.923	2.466					0.0060
		2.799	2.471					0.0061
		2.919	2.471					0.0061
			$\bar{d} = 2.468$					0.4849

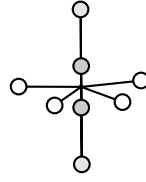


$\text{Ne}_7^+ (C_s)$	r	$R_1 - R_2$	$\frac{d_1 - d_3}{d'}$	E	ZPE	$E(\text{incl.}ZPE)$	$\Delta E(\text{eV})$	$charge$
$E_x^{HF} + E_c^{LYP}$	1.686	2.631	2.412	-901.628321	0.00384	-901.624484	0.0583	0.0072
			2.402					0.0076
			2.402					0.0076
			$\bar{d} = 2.405$					0.4636
			$d' = 3.142$					0.4636
								0.0252
$E_x^{HF} + E_c^{P86}$	1.677	2.967	2.451	-901.654024	0.00322	-901.650802	0.0367	0.0053
			2.466					0.0060
			2.466					0.0060
			$\bar{d} = 2.461$					0.4705
			$d' = 3.206$					0.4705
								0.0208

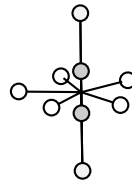
and locate only 4 and 5 neon atoms on the plane bisecting the ionic moiety, while placing two additional Ne atoms (which now have larger net charges and sit further away from the dimer midpoint) along the ionic axis. It is also interesting to see that $n = 9$ appears as a sort of “magic” number since the one-atom evaporation energy increases with respect to the other clusters. This result was also found by the latest DIM calculations [10].

In order to further extend the use of the DFT method, we also carried out some test calculations by treating both exchange *and* correlation within the DFT models, *i.e.* by simplifying the post-Hartree-Fock approach employed till now. The DFT variational calculations employed the Half and Half (HH) model, extensively discussed in the current literature (*e.g.* see [30,31]). The results are shown in Table 8 and largely confirm the previous findings in the

Table 7. Same computed quantities as in Table 6 but for the most stable configurations for Ne_8^+ (upper panel) and for Ne_9^+ (lower panel). See main text for the meaning of symbols.



$\text{Ne}_8^+ (C_s)$	r	$R_1 - R_3$	$\frac{d_1 - d_4}{d'}$	E	ZPE	$E(\text{incl.}ZPE)$	$\Delta E(\text{eV})$	$charge$
$E_x^{HF} + E_c^{LYP}$	1.685	2.623 2.639 2.624	2.418	-1030.541928	0.00438	-1030.537548	0.0565 0.0515	0.0071
			2.403					0.0086
			2.404					0.0085
			2.407					0.0073
			$\bar{d} = 2.408$					0.4589
			$d' = 3.142$					0.4589
$E_x^{HF} + E_c^{P86}$	1.675	2.937 2.911 2.872	2.472	-1030.571536	0.00359	-1030.567949	0.0367 0.0347	0.0062
			2.450					0.0057
			2.456					0.0058
			2.473					0.0062
			$\bar{d} = 2.463$					0.4673
			$d' = 3.207$					0.4673



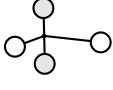
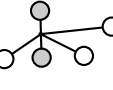
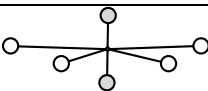
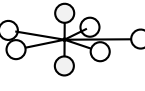
$\text{Ne}_9^+ (C_s)$	r	$R_1 - R_4$	$\frac{d_1 - d_5}{d'}$	E	ZPE	$E(\text{incl.}ZPE)$	$\Delta E(\text{eV})$	$charge$
$E_x^{HF} + E_c^{LYP}$	1.684	2.665 2.666 2.633 2.632	2.403	-1159.455684	0.00492	-1159.450765	0.0978 0.0831	0.0082
			2.393					0.0079
			2.392					0.0079
			2.403					0.0082
			2.411					0.0074
			$\bar{d} = 2.400$					0.4547
$E_x^{HF} + E_c^{P86}$	1.674	2.886 2.886 2.711 2.710	2.466	-1159.489167	0.00419	-1159.484979	0.0484 0.0320	0.0066
			2.454					0.0061
			2.455					0.0061
			2.466					0.0066
			2.481					0.0064
			$\bar{d} = 2.464$					0.4633
$d' = 3.206$	0.4633							

sense that the dimeric ion comes out to be the main ionic moiety of these clusters and the “shell-filling” process goes regularly into the bisecting plane from $n = 2$ up to $n = 5$, as shown before. Furthermore, the most stable structures show a more symmetric geometrical pattern with respect to the post-HF calculations of before: the distances between the neon atoms in the plane are all very close to

each other and close to the neutral dimer interaction minimum distance, as discussed before.

A sort of more global analysis of the behaviour of the small clusters discussed in the present work could be seen by looking at the departures from having a rigid ionic axis which are occurring along the series of larger structures. A simple view of the present results is shown in Figure 1,

Table 8. Computed geometries and positive charge for four different ionic clusters for which the optimized total energies and geometries were obtained within a full DFT treatment of exchange and correlation. The Half & Half modelling is the one discussed in reference [31].

half&half		r	R	d	charge
Ne_4^+		1.733	2.996	2.604	0.0031
				2.604	0.0031
				0.4969	0.4969
				0.4969	0.4969
Ne_5^+		1.733	2.999	2.613	0.0030
				2.604	0.0031
				2.604	0.0031
				0.4954	0.4954
Ne_6^+		1.732	3.009	2.612	0.0030
				2.612	0.0031
				2.604	0.0031
				2.603	0.4939
Ne_7^+		1.732	3.056	2.601	0.0031
				3.059	0.0031
				3.059	0.0031
				3.054	0.0031
			3.061	2.602	0.4923

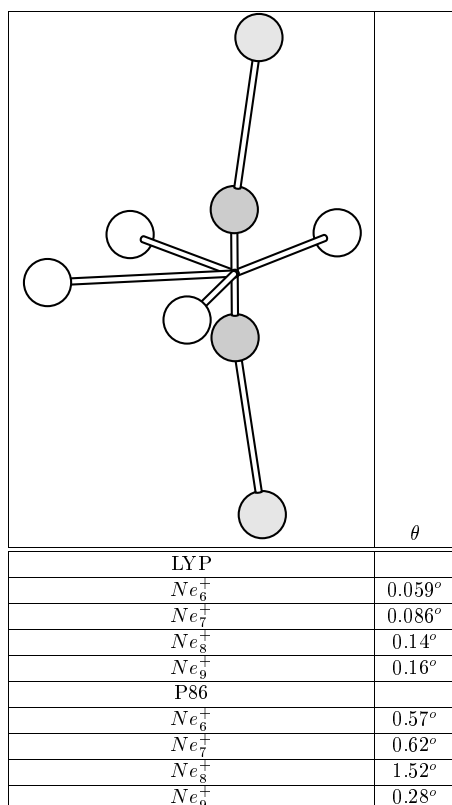


Fig. 1. Geometrical distortion of the principal axis along the ionic moiety, using the correlated calculations with E_c^{LYP} (LYP) and with E_c^{P86} (P86). The angles reported are the departure of the axis from the vertical positions ($\vartheta = 0^\circ$).

where we report the angle formed by the neon atoms along the axis: the angles shown in the table below that picture indicate the distortions from the perpendicular axis to the bisecting plane produced by the two choices of correlation corrections: E_c^{LYP} (LYP in the figure) and E_c^{P86} (P86 in the figure). One sees that the central ionic moiety, Ne_2^+ , is essentially along that axis and remains rigidly linear in Ne_6^+ and Ne_7^+ . On the other hand, when additional Ne partners are added along that axis (as it occurs in Ne_8^+ and Ne_9^+) we clearly see a more marked distortion (*away* from the planar atoms). A further display of the energetics along the series of examined clusters is shown in Figures 2 and 3, where we report several indicators of global cluster behaviour. Each figure refers to a different modelling for the correlation corrections: the E_c^{LYP} in Figure 2 and the E_c^{P86} in Figure 3.

The bottom panel in the figures show the changes of the Ne–Ne distances in the core moiety (lower line) among Ne atoms located in the bisecting plane (R values), of the distances of each neon atom in that same plane but from the ionic axis (d values) and the distances from the Ne atoms along the axis of the ionic core to the bisecting plane (d' values). For the series of systems examined we clearly see the appearance of a “shell” structure: the dimeric core remains nearly unperturbed during the cluster growth while the neon atoms on the bisecting plane place themselves at a distance from the ionic moiety which is further away but remains nearly constant with n . With the same token, those atoms also keep out of each other’s way (R values) because of the repulsive potentials between neutral dimers and essentially form slightly deformed neutral Ne_2 . Finally, the added atoms along the axis appear to locate themselves at distances from the moiety center

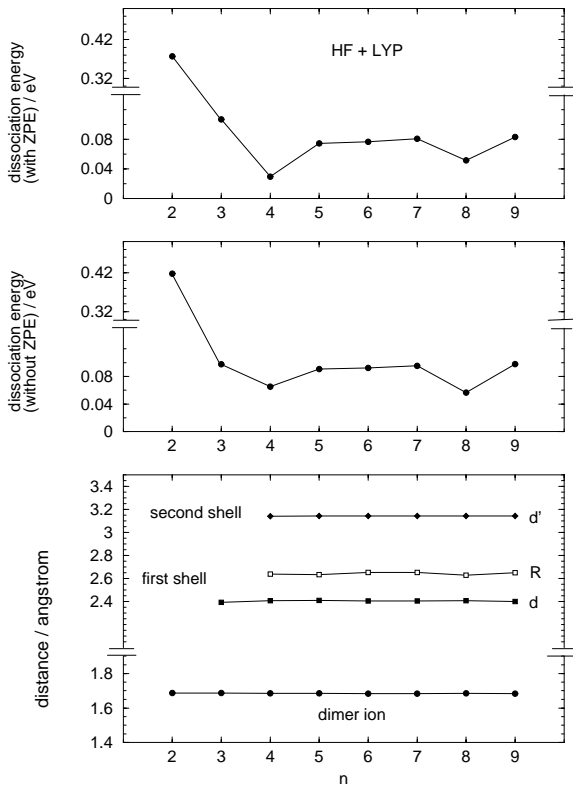


Fig. 2. Computed properties of the ionic clusters at the post-Hartree-Fock level with correlation corrections from E_c^{LYP} . Top panel: one atom dissociation energies with ZPE corrections (in eV) as a function of n . Middle panel: same quantities of above but without the ZPE correction. Bottom panel: relative distances, in each cluster, as a function of size n . All quantities in Å. See text for meaning of symbols.

larger than the ones of those Ne atoms lying in the plane and also carry very little positive charges. In other words, the present calculations show that all the cluster features obtained from DFT correlation corrections conjure up a physical picture whereby the ionic clusters chiefly maintain the dimeric moiety (that carries most of the cluster positive charge) as their clustering core. This result is even clearer when full DFT calculations of exchange and correlation effects are carried out for $4 \leq n \leq 7$ as reported in Table 8, where the HH modelling was employed [30,31].

The single-atom evaporative energies depicted in the middle panel of Figures 2 and 3 also tell us that marked differences exist between the values of such quantities depending on the specific location of the neon atom which undergoes evaporation. For example, when we do not include ZPE corrections, we find a marked drop from the value of the dimer break-up energy and those of all the additional neon atoms. This is in keeping with experiments [47] in spite of the fact that our calculations give the former energy as too small while correctly reproducing the latter values.

Both treatments of correlation corrections, in fact, show that the dissociation energy reduces by a factor of ten at least when $n > 2$ is considered. In spite of the fact

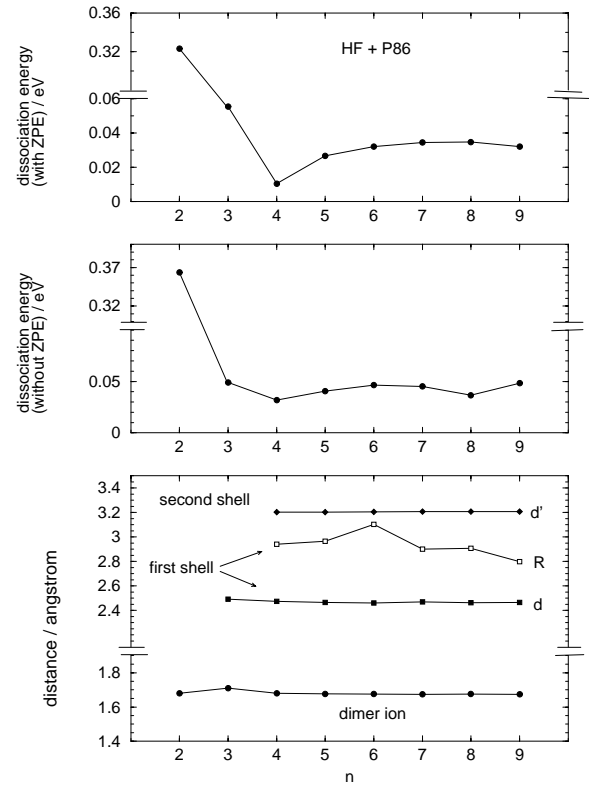


Fig. 3. Same computed quantities as in Figure 2 but using the E_c^{P86} correlation discussed in the main text. See there for the meaning of symbols.

that the DFT corrections strongly underestimate the Ne_2^+ dissociation energy (see before), the present calculations however indicate nearly constant values for single-atom evaporation energies in the smaller clusters. The same result is found when the calculations further include ground state vibrational effects through zero-point-energy corrections (top panels in Figs. 2 and 3).

Another interesting feature regarding the last effect, *i.e.* the harmonic model for quantum features of the partner locations within the bound clusters, can be seen from the results reported in Figure 4. What we show there is the behaviour of the computed ZPE values, in units of cm^{-1} , as a function of the number n of atoms in the cluster.

Both post-HF calculations show a steady increase of such values from about 300 cm^{-1} for Ne_2^+ up to about 1000 cm^{-1} for Ne_9^+ . The addition of each of the new partners, therefore, does not imply a linear growth of the total contribution. The vibrational model of the linear trimer, for instance, corresponds to four normal coordinates while 21 of them are present in Ne_9^+ , an increase of about 5.2. The corresponding *total* increase of the delocalization effect when going from the trimer to the Ne_9^+ corresponds to an energy increase of a factor of about 3.2. Hence, we see that larger clusters are, as expected, correspondingly more “compact” objects than the smaller ionic clusters.

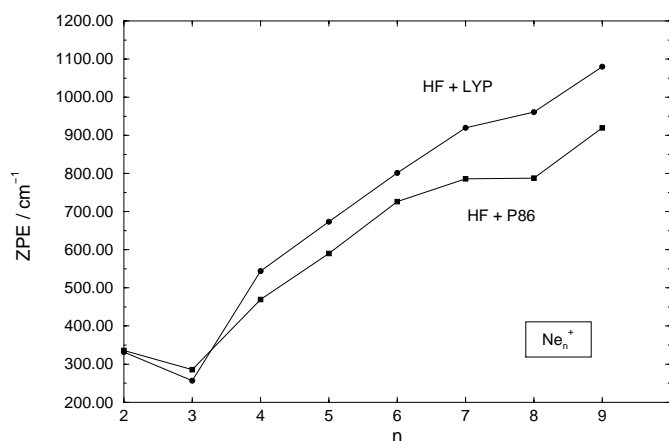


Fig. 4. Computed Zero-Point-Energy (ZPE) corrections as a function of size n and for two different DFT models for the correlation energy corrections. All values in cm^{-1} . See text for the meaning of symbols.

4 Present conclusions

With the work described in the previous section we have analysed in some detail the energetics and the likely structures of ionized neon clusters containing up to nine atomic partners. Given the fact that the existing previous calculations [9,10] had employed DIM methods for constructing the full interaction, thereby using as building blocks the diatomic Hamiltonians for the ions and for the neutrals, we decided to try instead an all-electron treatment that employed the full Hamiltonian of each n -atom system. On the other hand, to render the calculations more amenable to completion, we have treated the full variational problem first at the Hartree-Fock level and then have repeated the variational calculations to generate correlated Molecular Orbitals (MO's) by using correlation energy corrections, E_c , from a Density Functional modelling. Different models have been employed and quantitative differences were found among them on the values of total binding energies, geometry details and total electronic energies, as shown in Tables 1–7. On the other hand, the qualitative picture that emerges in our calculations is very similar from all the DFT treatments and allows us to draw the following conclusions:

- (i) all the calculations appear to indicate that the ionic neon clusters are built around a fairly localized charge distribution. In particular, the diatomic ion is found to carry more than 90% of the positive charge in each cluster;
- (ii) the additional neon atoms beyond $n = 2$ are found, initially, to place themselves on a plane bisecting the axis containing the ionic moiety. This feature occurs up to five atoms in that plane (Ne_7^+);
- (iii) the above additional Ne atoms are found to be nearly neutral partners and to largely remain at relative distances from each other which are similar to that of the isolated, neutral dimer which is around 3 \AA . Thus, our calculations place the additional Ne as equivalent partners distanced by about $2.8\text{--}3.0 \text{ \AA}$;

- (iv) the further growth of these small clusters appears to occur by locating the additional Ne atoms into a third “shell” along the axis of the ionic moiety. In other words, from $n > 7$ we see that the placement of two neon partners along the axis is preferred to having only one atom there and four or five others located on the bisecting plane discussed before;
- (v) the effect from quantum delocalization was also examined, in a simplified manner, by evaluating zero-point-energies (ZPE's) within the harmonic approximation. It was indeed found to be important and to markedly lower the energetics for the single-atom evaporative process. On the other hand, the present calculations also show that the larger clusters tend to become more compact in the sense that quantum contributions from each added atoms do not remain constant but decrease as n increases.

Some of the above considerations are in line with what has been found before [9] and also in part, with the more recent DIM calculations [10]. In the latter case the most striking difference is the absence, in our calculations, of the presence of a tetrameric ion as the main cluster growth moiety. On the other hand, the present DFT calculations appear to have difficulties in estimating Ne_2^+ binding energies correctly and therefore might overestimate the correlation effects in the ionic species, thereby limiting the delocalization of the initial charge to the dimeric moiety. Similar Coupled Cluster (CC) calculations [30,52] have no difficulty in yielding the correct dimeric dissociation energy but still find the positive charge chiefly localized on the latter species.

In conclusion, the ionic clusters studied here are found to be, once more, very different objects from their neutral counterparts [55] and to favour the formation of growth shells of atoms around a central ionic moiety which carries the great majority of the existing positive charge. We are currently revisiting this problem by using fully quantum treatments for the nuclear motion in order to see more specifically the expected “floppy” nature of such clusters, as we have already found in the case of protonated helium clusters [56].

The financial support of the Italian Ministry for University and Research (MURST), of the Research Committee of the University of Rome and the Supercomputing Consortium (CASPUR) are gratefully acknowledged.

References

1. M.R. Hoare, *Adv. Chem. Phys.* **40**, 49 (1979); M. Amarouche, G. Durand, J.P. Malrieu, *J. Chem. Phys.* **88**, 1010 (1988); H.U. Bohmer, S.D. Peyerimhoff, *Z. Phys. D* **11**, 239 (1989).
2. T.J. Beck, J.D. Doll, D. Freeman, *J. Chem. Phys.* **90**, 5651 (1990).
3. D.J. Wales, R.S. Berry, *J. Chem. Phys.* **92**, 4283 (1990).
4. I. Last, T.F. George, *J. Chem. Phys.* **98**, 6406 (1993).
5. K. Norwood, J.-H. Guo, C.Y. Ng, *J. Chem. Phys.* **90**, 2995 (1989).

6. M. Rosi, C.W. Bauschlicher, *Chem. Phys. Lett.* **159**, 479 (1989).
7. J. Hesslich, P.J. Kuntz, *Z. Phys. D* **2**, 551 (1990).
8. F.A. Gianturco, P. De Lara-Castells, F. Schneider, *Chem. Phys. Lett.* **259**, 641 (1996).
9. M. Fieber, A.M. Ding, P.J. Kuntz, *Z. Phys. D* **23**, 171 (1992).
10. F.Y. Naumkin, D.J. Wales, *Mol. Phys.* **93**, 633 (1998).
11. J.C. Slater, *Self-Consistent-Fields for Atoms and Molecules* (Mc Graw Hill, New York, 1987).
12. N.M. March, *Self-Consistent-Fields in Atoms* (Oxford U.P., 1985).
13. D. Bohm, *Phys. Rev.* **85**, 166 (1952).
14. W. Kohn, L.J. Sham, *Phys. Rev. A* **140**, 1133 (1965).
15. P.C. Hohenberg, W. Kohn, *Phys. Rev. B* **136**, 864 (1964).
16. A.D. Becke, *J. Chem. Phys.* **98**, 5648 (1993) and references therein.
17. P. Gombas, *Die Statistische Theorie des Atoms und ihre Anwendungen* (Springer Verlag, Berlin, 1949).
18. A.D. Becke, *Phys. Rev. A* **38**, 3098 (1988).
19. A.D. Becke, *J. Chem. Phys.* **96**, 2155 (1992).
20. A.D. Becke, *J. Chem. Phys.* **97**, 9173 (1992).
21. J. Harris, *Int. J. Quant. Chem. Symp.* **13**, 189 (1979).
22. F.A. Gianturco, J.A. Rodriguez-Ruiz, *J. Mol. Struct. Theochem.* **260**, 99 (1992).
23. C. Lee, W. Yang, R.G. Parr, *Phys. Rev. B* **37**, 785 (1988).
24. F.A. Gianturco, J.A. Rodriguez-Ruiz, *Phys. Rev. A* **47**, 1075 (1993).
25. J.P. Perdew, A. Zunger, *Phys. Rev. B* **23**, 5048 (1981).
26. J.P. Perdew, *Phys. Rev. B* **33**, 8822 (1986).
27. S.H. Vosko, L. Wilk, M. Nusair, *Can. J. Phys.* **58**, 1200 (1980).
28. D.H. Ceperley, *Phys. Rev. B* **18**, 3126 (1990).
29. J.P. Perdew, Y. Wang, *Phys. Rev. B* **45**, 13244 (1992).
30. GAUSSIAN 94 (Revision D.1), M.J. Frisch, G.W. Trucks, H.B. Schlegel, P.M.W. Fill, B.G. Johnson, M.A. Robb, J.R. Cheeseman, T.A. Keith, G.A. Petersson, J.A. Montgomery, K. Raghavachari, M.A. Al-Laham, V.G. Zakrzewski, J.V. Ortiz, J.B. Foresman, J. Cioslowski, B.B. Stefanov, A. Nanayakkara, M. Challacombe, C.Y. Peng, P.Y. Ayala, W. Chen, M.W. Wong, J.L. Anders, E.S. Replogle, R. Gomperts, R.L. Martin, D.J. Fox, J.S. Binkley, D.J. Defrees, J. Baker, J.P. Stewart, M. Head-Gordon, C. Gonzalez and J.A. Pople, Gaussian, Inc., Pittsburgh PA, 1995.
31. F.A. Gianturco, F. Paesani, in *Conceptual Perspectives in Quantum Chemistry*, edited by J.L. Calais, E. Kryachko (Kluwer Acad. Publ., 1997), p. 337.
32. F.A. Gianturco, F. Filippone, *Chem. Phys.* **241**, 203 (1999).
33. H. Haberland, *Surf. Sci.* **156**, 305 (1985).
34. J.J. Saeng, M. Soler, N. Garcia, *Surf. Sci.* **156**, 120 (1985).
35. I. Last, T.F. George, *J. Chem. Phys.* **93**, 8925 (1990).
36. J. Cizek, *Adv. Chem. Phys.* **14**, 35 (1969).
37. H. Hogreve, *Chem. Phys. Lett.* **215**, 72 (1993).
38. J.S. Cohen, B. Schneider, *J. Chem. Phys.* **61**, 3240 (1974).
39. R.S. Mulliken, *J. Chem. Phys.* **52**, 5170 (1970).
40. R.G. Keese, A.W. Castleman, *J. Phys. Chem. Ref. Data* **15**, 1011 (1986).
41. H.-J. Werner, P.J. Knowles, J. Almlöf, R.D. Amos, S.T. Elbert, W. Meyer, E.-A. Reinsch, R.M. Pitzer, A.J. Stone, P.R. Taylor, Molpro, a package of *ab initio* programs.
42. E. Buonomo, M.P. De Lara, S. Miret-Artés, G. Delgado-Barrio, F.A. Gianturco, P. Villarreal, *Chem. Phys.* **218**, 71 (1997).
43. F.A. Gianturco, M.P. De Lara-Castells, F. Schneider, *J. Chem. Phys.* **106**, 7586 (1997).
44. F.X. Gadea, M. Amarouche, *Chem. Phys.* **140**, 385 (1990).
45. T. Ikegami, T. Kondow, S. Iwata, *J. Chem. Phys.* **99**, 3588 (1993).
46. *E.g.* see H. Haberland, T. Kolar, C. Ludewigt, A. Risch, M. Schmidt, *Z. Phys. D* **20**, 33 (1991).
47. *E.g.* see K. Hiraoka, T. Mori, *J. Chem. Phys.* **92**, 4408 (1990).
48. W.R. Wadt, *Appl. Phys. Lett.* **38**, 1030 (1981).
49. F.Y. Naumkin, P.J. Knowles, J.N. Murrell, *Chem. Phys.* **193**, 27 (1995).
50. D.J. Wales, J.P.K. Doye, *J. Phys. Chem. A* **101**, 5111 (1997).
51. T.H. Dunning, P.J. Hay, *Modern Theoretical Chemistry*, edited by H.F. Schaefer (Plenum, New York, 1979), Vol. III.
52. F.A. Gianturco, F. Sebastianelli, in preparation.
53. U. Kleinekathofer, K.T. Tang, J.P. Toennies, C.L. Yiu, *J. Chem. Phys.* **107**, 9502 (1997).
54. F.A. Gianturco, F. Filippone, *Europhys. Lett.* **44**, 585 (1998).
55. *E.g.* see I.F. Silvera, *Rev. Mod. Phys.* **52**, 393 (1980).
56. B. Balta, F.A. Gianturco, F. Paesani, *Chem. Phys.* (in press, 2000).